IOP Publishing

Radiation Detection for Nuclear Physics
Methods and industrial applications
David Jenkins

Chapter 9

Neutron detectors

This chapter provides an overview of the most commonly encountered technologies used in both fast and thermal neutron detection. In terms of fast-neutron detection, organic scintillators are the most commonly employed technology. The physical principles behind organic scintillators are reviewed, leading to an explanation of how they can distinguish neutrons from gamma rays on the basis of the fast and slow components of the scintillation light. Different types of organic scintillator are reviewed, focussing on liquid scintillators and plastic scintillators which are largely used for fast neutron counting and neutron time-of-flight measurements, respectively. Attention then turns to thermal neutron detectors, which operate on rather different principles: using nuclear reactions on light nuclei to produce charged particles, which can ionise a gas or produce scintillation light. The classic detector technology for thermal neutron detection is a ^{3}He gas-filled proportional counter. The scarce availability and high price of ^{3}He has focussed attention more recently on alternatives using different neutron-converter materials such as ^{6}Li and ^{10}B. The principles behind such detectors are reviewed.

Concepts: Organic scintillators: liquid scintillators and plastic scintillators; fast neutron discrimination; neutron detector arrays; thermal neutron detection; ^{3}He tubes; ^{3}He alternatives based on ^{6}Li or ^{10}B; societal applications of thermal neutron detection

9.1 Fast neutron detectors

Fast neutrons are produced in fission, by certain specialist radioactive sources and in nuclear reaction studies in the laboratory (see section 3.5). Fast neutrons are not themselves ionising and so fast neutron detection chiefly relies on transferring some of the neutron's kinetic energy to a charged particle which is itself ionising. The largest energy transfer possible, kinematically speaking, is with a proton since the proton and neutron have a near-identical mass. Neutrons scattering off heavy nuclei

doi:10.1088/978-0-7503-1428-2ch9

will only impart a small amount of energy[1]. These considerations explain why most fast neutron detectors are based on the principle of proton (or in some cases, deuteron)-recoil. An ideal detector, therefore, would be a hydrogen-rich scintillator material and this is the class of *organic scintillators*, outlined in section 4.3.2 and revisited in more detail here. Reviews of the functionality of organic scintillators may be found in the monograph of J B Birks [1] and elsewhere, e.g. [2]. Organic scintillators come in a variety of forms including *organic crystals*, *liquid scintillators* (see section 9.1.1) and *plastic scintillators* (see section 9.1.2). The earliest organic scintillators were crystals such as anthracene and stilbene. These have fast decay time of the order of 10 ns. However, they cannot be readily machined and historically, were difficult to obtain in large sizes, although more recent methods have started to surmount this obstacle [3]. Accordingly, their use has been somewhat limited. Moreover, their light emission is anisotropic [3]. Nevertheless, anthracene is the brightest, i.e. highest light output per unit deposited energy of traditional organic scintillators, corresponding to 17 400 photons MeV^{-1}, and so it is common for organic scintillators to have their performance expressed as % anthracene.

Quenching in organic scintillators

An interesting feature of organic scintillators is *quenching*[2]. Where scintillator excitation centres are spaced far apart and interaction between them is minimal, then it can be shown for particles with a low stopping power, e.g. electrons above 100 keV that the yield of scintillation light, L, in an organic scintillator is proportional to the energy deposited i.e.

$$\frac{\mathrm{d}L}{\mathrm{d}r} = S\frac{\mathrm{d}E}{\mathrm{d}r}, \tag{9.1}$$

where S is the scintillation efficiency. This is not the case for heavily ionising particles, e.g. protons, α-particles, heavy ions where the light output is quenched according to Birks' law [4]:

$$\frac{\mathrm{d}L}{\mathrm{d}r} = S\frac{\frac{\mathrm{d}E}{\mathrm{d}r}}{1 + kB\frac{\mathrm{d}E}{\mathrm{d}r}}, \tag{9.2}$$

where kB is Birks' constant comprising k, the energy transfer probability and B, a constant of proportionality associated with the number of damaged molecules [5]. This relationship breaks down for particles with a very high linear energy transfer (LET) because it does not explicitly account for the spatial configuration of the fluorescent and damaged molecules [5]. Figure 9.1 shows the strong deviation from linearity in light yield for high LET ions, implied by Birk's law.

These considerations regarding the quenching of scintillators by transiting ions, i.e. equation (9.2), lead to the useful concept of electron equivalent energy,

[1] Imagine comparing the collisions of two equal mass snooker balls to a collision between such a snooker ball and a medicine ball.

[2] It is not clear how applicable this is to inorganic scintillators.

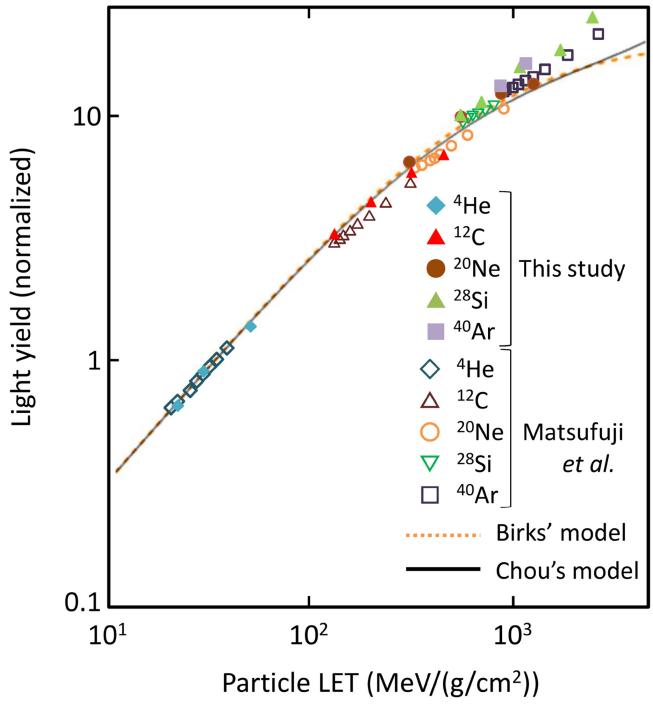

Figure 9.1. Light yield from an NE-102A organic liquid scintillator detector irradiated by heavy ions (150–550 MeV/u) as a function of linear energy transfer (LET). The dashed line is the Birk's model discussed in the text which deviates from the data at the highest values of LET. (Reprinted from [5] with permission from PLOS under Creative Commons License.)

commonly written as keV_{ee} or MeV_{ee} this notation will be seen extensively in some of the figures presented in this chapter.

Potential for neutron-gamma discrimination

The excitation and decay modes of organic scintillators naturally lend them to the task of neutron-gamma ray discrimination. In practice, this translates into the differing manner in which recoil protons and photoelectrons/Compton scattered electrons interact in material (see chapter 2). A gamma ray interacts discontinuously in a material transferring its energy to one or a few photoelectrons or Compton-scattered electrons, whereas an ion such as a proton, alpha particle or heavy ion deposits energy all along its track and the effective $\frac{dE}{dx}$ is large. The excitation densities in an organic scintillator are correspondingly higher for the interaction of recoil protons from a neutron interaction. This leads to a suppression of the singlet, i.e. fluorescence decay mode and an enhancement of the triplet, i.e. phosphorescence decay mode. The net effect of this is to enhance the long-lived component of the scintillation light relative to the short-lived component. Figure 9.2 (bottom) shows the effect of this mechanism on the components of the scintillation light for three common organic crystals: anthracene, stilbene and P-terphenyl. In the data analysis,

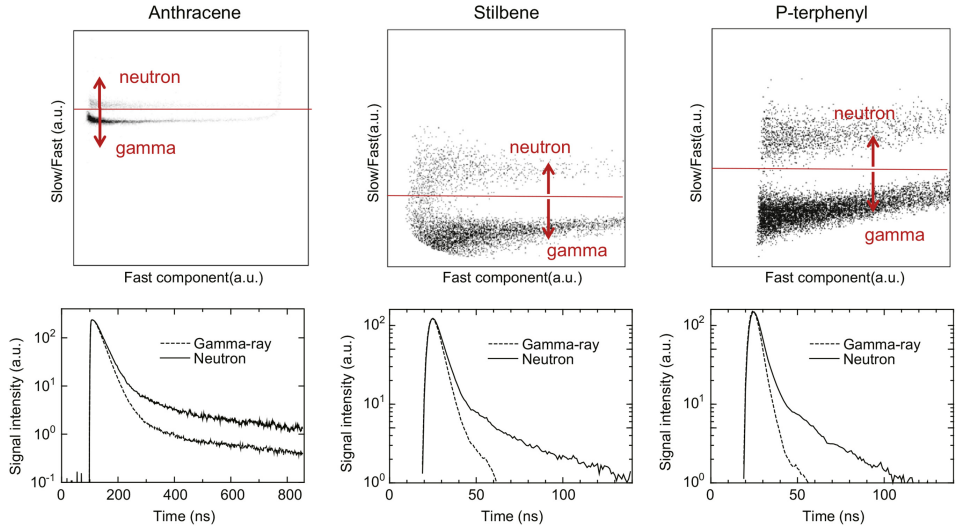

Figure 9.2. Neutron/gamma-ray discrimination using anthracene, stilbene and P-terphenyl. The neutrons are from a ^{252}Cf source and the gamma rays from a ^{60}Co source. (Bottom) the scintillation decay spectrum for neutrons and gamma-rays for each of the three materials. (Top) discrimination of neutrons from gamma rays using the ratio of the slow/fast components plotted against the fast component. In each case, the corresponding slow/fast windows were: 20–40 and 40–150 ns (anthracene), 20–40 and 40–150 ns (stilbene) and 20–30 and 30–150 ns (P-terphenyl). (Reprinted from [6] with the permission of Elsevier.)

windows may then be set on the different fast and slow components of the light output to discriminate neutrons from gamma rays (see figure 9.2 (top)).

9.1.1 Liquid scintillator detectors

Liquid scintillator detectors typically comprise a detector volume with a metal can containing an organic liquid scintillator. The can usually has a bellows arrangement to allow for expansion of the liquid under change of temperature. The cans have optical windows in them to allow coupling to a PMT. Typical liquid scintillators need to be handled with care; depending on the choice of liquid it may be harmful and carcinogenic, and it may also have a low flash point. The classic liquid scintillator material is BC501A. It has a decay time of 3.2 ns and a peak wavelength of 425 nm.

Liquid scintillator detectors are conventionally employed as fast neutron counters since they usually have no particular sensitivity to the incident neutron energy. They are often installed as arrays replacing some portion of a germanium detector array to provide fast neutron detection. An example of a contemporary liquid scintillator neutron array is the NEDA array (see figure 9.3) designed to be used at the SPIRAL2 facility in Normandy, and elsewhere. A related example is the DESCANT neutron array at TRIUMF (see figure 9.4) which is a variant of the standard approach since it makes use of deuterated liquid scintillator [7]. The n–d scattering reaction is asymmetric in the centre-of-mass as the neutron and deuteron have different masses. This means that the pulse-height information recorded from a deuterated scintillator

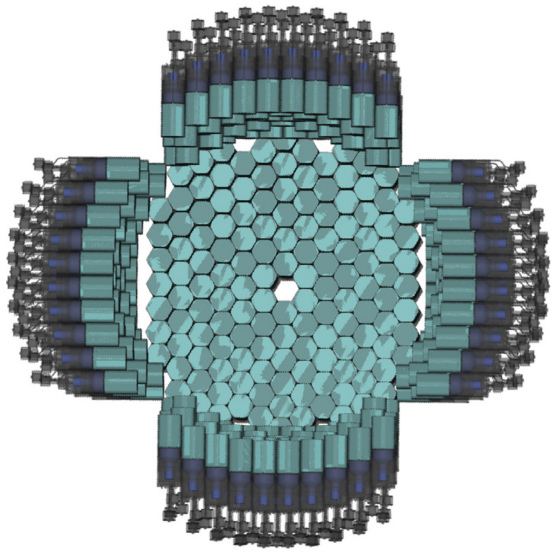

Figure 9.3. 3D CAD drawing of the NEDA array with a 2π solid angle coverage at a distance of 1 m. This full design comprises 331 individual identical detectors. (Reprinted from [8] with the permission of Elsevier.)

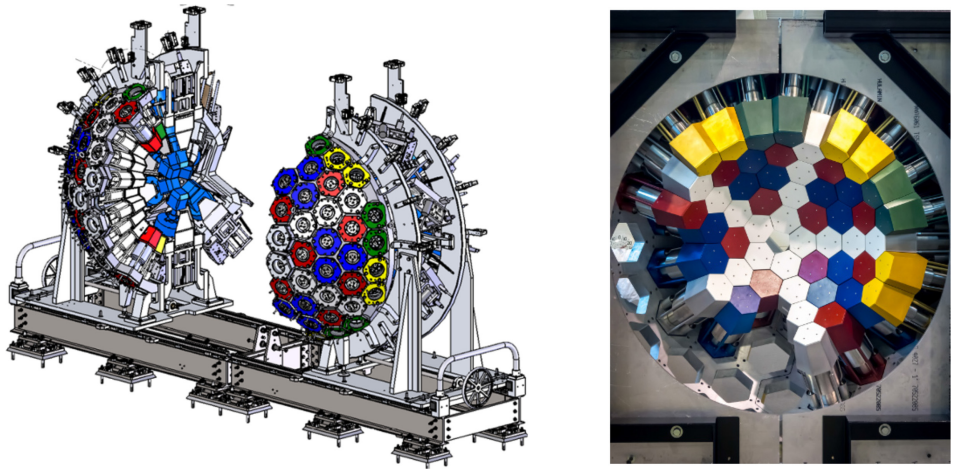

Figure 9.4. The DESCANT neutron array: (left) CAD drawing of DESCANT coupled to the GRIFFIN germanium detector array and (right) partially assembled DESCANT array. (Reprinted from [9] with the permission of Elsevier under Creative Commons License.)

detector, such as those making up DESCANT, is sensitive at some level to the incident neutron energy (see figure 9.5).

Principles of neutron discrimination with liquid scintillators

In typical in-beam nuclear physics experiments, neutrons and gamma rays may both be produced, which leads to ambiguity in the signal recorded in liquid scintillator

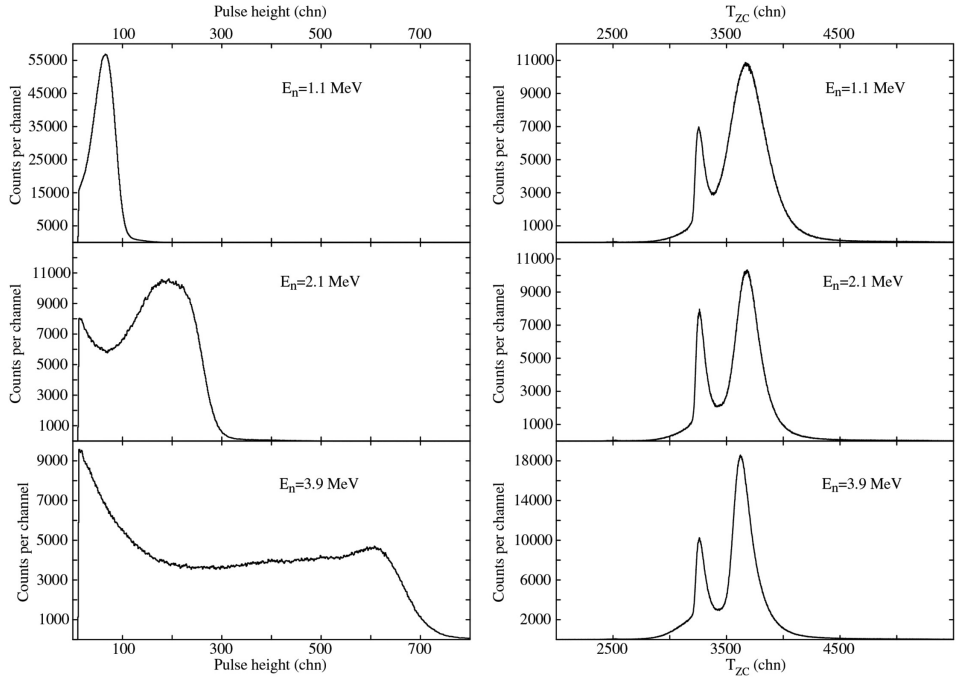

Figure 9.5. Pulse height (left) and neutron-gamma discrimination (right) for a DESCANT detector using monoenergetic neutrons of 1.1 MeV (top), 2.2 MeV (middle) and 3.9 MeV (bottom). (Reprinted with the permission of [10] under Creative Commons License.)

detectors as such detectors respond to both types of indirectly ionising radiation. However, neutrons can be discriminated in two ways. First, the time-of-flight for neutrons and gamma rays is different since gamma rays travel at the speed-of-light but typical fast neutrons (~MeV) travel only at a small fraction of the speed-of-light. If the production time can be well defined, e.g. an accelerated beam is pulsed with a pulse-width of order nanoseconds then the difference in time-of-flight between reaction target and the neutron detector can be used to discriminate. An example of neutron separation by time-of-flight is shown in figure 9.6 for ~2 MeV neutrons and gamma rays over a flight distance of around 5 m. The second technique is to discriminate neutrons from gamma rays using pulse shape analysis. This relies on neutrons generating a different response in the liquid scintillator leading to more amplitude in the tail of the pulse, as described in section 4.3.2. This can be exploited both using analogue electronics, splitting the signal into fast and slow components, as was achieved with the EUROBALL neutron wall [11] and with digital electronics as in the example of the more recent NEDA array [8]. Figure 9.7 shows an example of making use of this effect to discriminate neutrons from gamma rays. In practice, where both time-of-flight and pulse-shape analysis are available then they are applied in conjunction leading to a very high rejection of gamma rays and robust identification of fast neutron events.

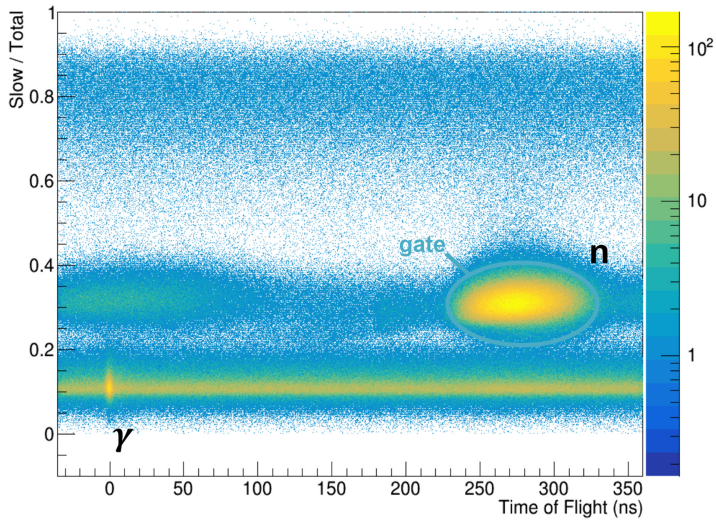

Figure 9.6. Discrimination of fast neutrons from gamma rays using a NEDA detector: the fraction of the slow component to total plotted against time of flight. The fast neutrons are well-localised.

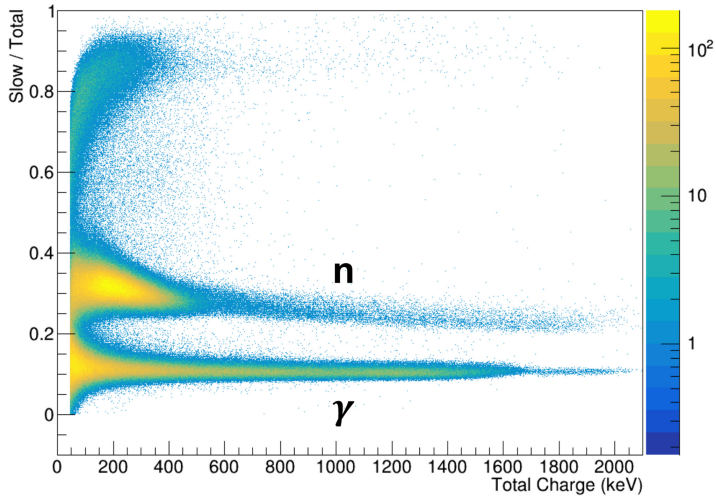

Figure 9.7. Neutron discrimination using NEDA: the fraction of the slow component to total plotted against total.

Complications enter the analysis of data from liquid scintillator arrays when it is required to identify two discrete neutron interactions. This is because neutrons interact predominantly through elastic and inelastic scattering and so may scatter out of one detector and into another leading to the detection of two 'neutron events' originating from the same neutron. A possible route to separation of such scattered events is to look at the time distribution of the interactions, however, this may not completely resolve the ambiguity. Figure 9.8 provides an example of Monte Carlo

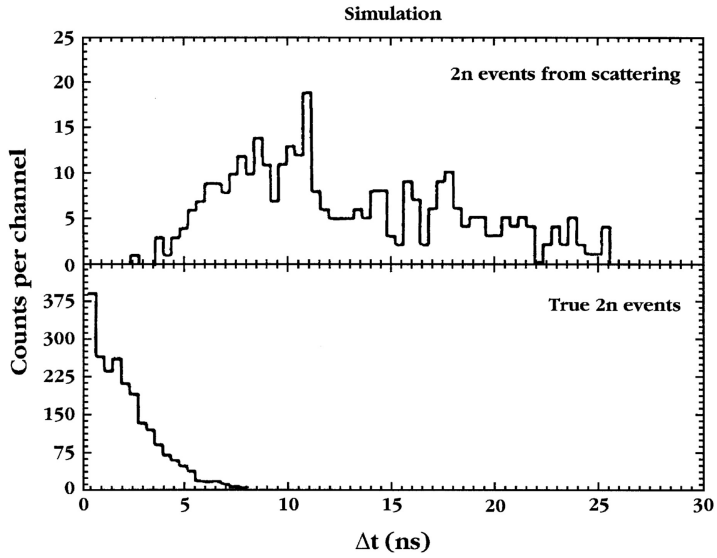

Figure 9.8. Monte Carlo simulation of time distributions from direct hits and scattered neutrons in the NORDBALL neutron wall. (Reprinted from [11] with the permission of Elsevier.)

simulation of the time distribution of direct neutron hits and such neutron scatters, which illustrates the experimental difficulty.

9.1.2 Plastic scintillator detectors

Plastic scintillators are a relatively inexpensive detector technology which is efficient for fast neutron detection. Here, the generation of scintillation light is initiated by the recoil of protons in the hydrogen-rich material. Plastic scintillators are characterised by relatively low light output but their chief advantage is their fast time response with rise times of order 1 ns and decay times of a few ns. This means that plastic scintillator detectors can count very fast and are also excellent for neutron/gamma discrimination based on time-of-flight. Due to its low effective Z, gamma ray interactions in plastic scintillator are predominantly associated with Compton scattering, which means they are not practical as spectroscopic gamma ray detectors but are useful for quantifying gamma flux or to provide a coincidence signal.

Plastic scintillators are usually based on a standard plastic matrix incorporating aromatic molecules such as polyvinyltoluene (PVT) or polystyrene (PS). Such plastics on their own are fluorescent but the light yield is extremely low. Moreover, the light emission is typically in the near-UV (300–350 nm) and such plastics re-absorb this light meaning the mean-free path of the scintillation light is very low (of order millimetres) and the decay time for light emission of, e.g. PS, is around 16 ns [12]. In order to achieve more useful properties such as a longer attenuation length and fast decay time, plastic scintillators typically have primary fluors incorporated into them at the level of about 1% by weight. Non-radiative

energy transfer, known as *Fortster transfer* can occur between the plastic molecules and the primary fluor. This leads to a significantly higher light yield with emission of scintillation light at longer wavelengths than the base plastic (see figure 9.9). Moreover, the attenuation length for the light emitted by the fluors is of order 10 cm so scintillation light can be more readily extracted from a plastic scintillator with a useful volume.

In order to extend the attenuation length of plastic scintillators and shift the peak wavelength of light emission to match with different choices of photosensor, a wavelength shifter material is frequently added at the level of around 0.01% by weight. The inclusion of different fluors and wavelength shifter can be tuned to produce plastic scintillator with a variety of wavelength-emission characteristics (see figure 9.10). Standard plastic scintillators have peak emission around 400–430 nm which is well matched to the response of SiPMs, for example. Typical light emission from plastic scintillators is of the order of 10 000 photons MeV^{-1}. There are many suppliers of plastic scintillator but a good idea of what is available in terms of plastic scintillators with different wavelength emission, decay time etc, is available from ELJEN.

Plastic scintillator can be cast and machined like normal plastics allowing large and/or complex pieces to be created. It can also be produced in the form of scintillating fibres. Indeed, recently, there have been the first attempts to 3D print plastic scintillator [15], although the material produced has yet to reach the quality in terms of light output etc of conventionally produced materials. Nevertheless, this

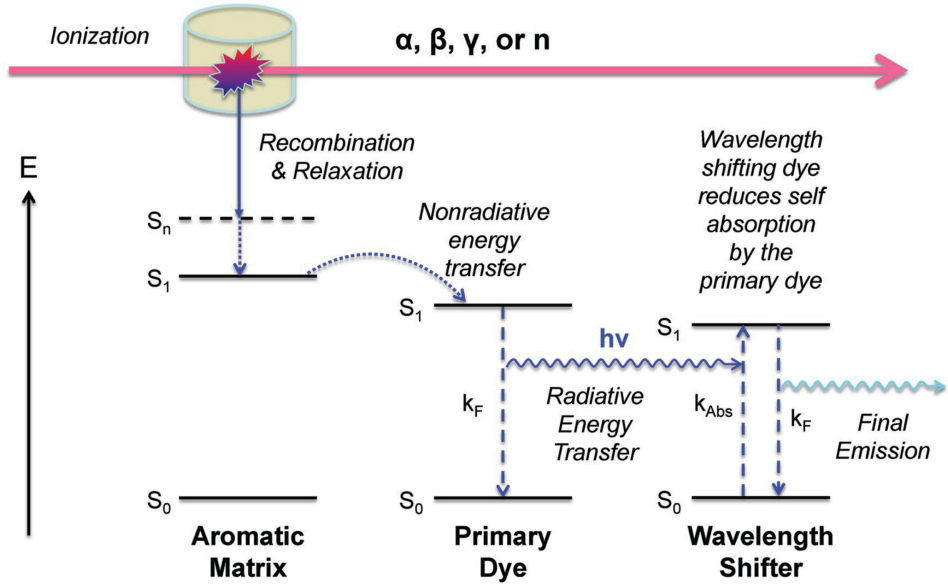

Figure 9.9. Physical processes in scintillation of organic materials. (Reprinted from [13] with permission from Wiley.)

Figure 9.10. Plastic scintillators with different wavelength emission when illuminated with ultraviolet light. (Reprinted from [14] with the permission of Elsevier under Creative Commons License.)

is clearly an area to watch as it should offer great flexibility and ease of design of prototypes.

Plastic scintillator can be formed into bars, rods, thin sheets or other planar geometries. It is readily connected to a variety of light sensors such as PMTs and SiPMs. An alternative to the regular approach of collecting light on a face is to machine grooves or channels into a slab of plastic scintillator and run optical fibres down these channels to collect the light and transport it to light sensors mounted at some distance away. Depending on the wavelength matching of the light emission of the plastic and the light sensor employed, sometimes wavelength-shifting optical fibres are employed to provide better wavelength matching to the light sensor.

Plastic scintillator can also be doped at the few % level with high-Z materials [13] such as tin or lead [16] to make them more efficient for gamma rays. Here, the improvement arises from increased probability for photoelectric absorption on the high-Z inclusions. Plastic scintillator may also be doped with gadolinium to turn it into a thermal neutron detector—an application more fully described in section 9.2.2.

Examples of neutron detector arrays based on plastic scintillator include VANDLE [17] constructed at Oak Ridge National Laboratory which is intended for studies of beta-delayed neutron emission (see figure 9.11) and nuclear reaction studies where the outgoing particle is a neutron. VANDLE comprises long bars of plastic scintillator coupled to PMTs on both ends. VANDLE is coupled to a digital data acquisition system based on Pixie-16 modules from XIA [17]. Other examples include NeuLAND [18] intended for the FAIR facility in Darmstadt, Germany.

Neutron-discriminating plastic scintillator

Plastic scintillators, e.g. EJ-276, are currently becoming available that offer pulse-shape discrimination between fast neutrons and gamma rays [19]. Figure 9.12 illustrates the capability to distinguish clearly between fast neutron and gamma ray interactions with such materials with a comparable performance to that of a standard liquid scintillator. Clearly the solid nature of the plastic offers significant advantages over liquid scintillators and none of the related hazards discussed above.

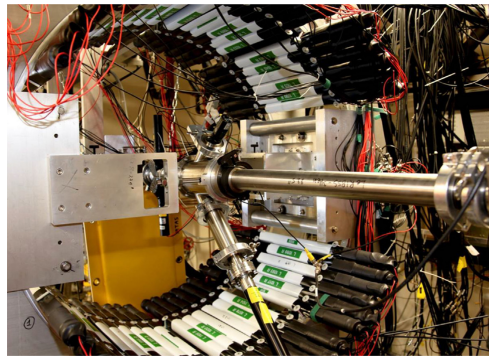

Figure 9.11. Photograph of the VANDLE neutron array arranged for study of beta-delayed neutrons comprising 48 individual modules. (Reprinted from [17] with the permission of Elsevier.)

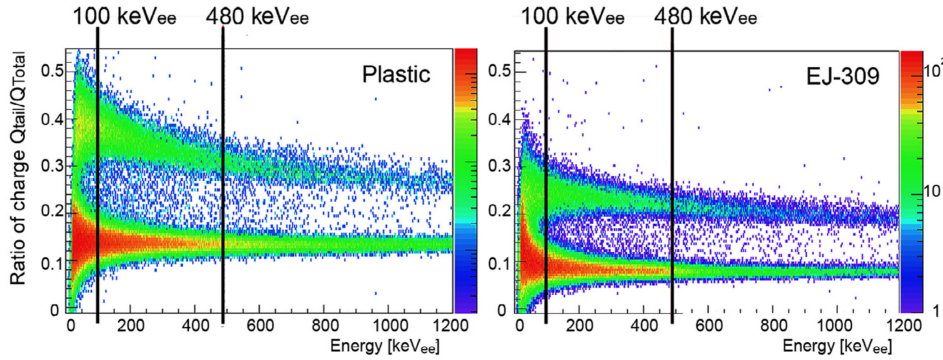

Figure 9.12. Neutron-gamma discrimination using plot of the ratio of charge in the tail of the pulse to total against electron-equivalent energy: (left) using 50 mm diameter, 76 mm long PSD plastic, and (right) using a liquid scintillator (EJ-309) of the same dimension. (Reprinted from [19] with the permission of Elsevier.)

In the longer term, this has significant potential for use in experimental nuclear physics and in application areas.

9.1.3 Emerging alternatives for fast neutron detection

Inorganic scintillator detectors

As noted in section 5.2.1, there are a number of inorganic scintillator detectors, e.g. CLYC and CLLBC, which can function as dual-purpose gamma-ray/fast neutron detectors; a critical review can be found here [20]. This functionality commonly depends on chlorine content in the crystal composition, where neutrons interact via the ^{35}Cl(n,p) reaction. Such detectors are relatively small, however, and expensive. The neutron detection efficiency is also rather low. For these reasons, they are yet to be widely adopted in experimental nuclear physics although they are undoubtedly valuable in nuclear security applications, chiefly because they can provide gamma-ray and neutron detection in a single compact unit.

^{4}He scintillation detectors

There is significant potential for liquid or gaseous ^{4}He-based scintillator detectors for fast neutron detection[3] [21, 22]. ^{4}He is a good scintillator emitting in the UV region, $\lambda\sim$ 80 nm. A typical implementation would be to have a gas-filled tube of ^{4}He with the walls of the tube covered with reflective material and a wavelength shifting phosphor that converts the scintillation photons to 430 nm so they can be more suitably recorded by PMTs at the two ends of the tube [22].

Since ^{4}He is a relatively light nucleus it can recoil in a neutron-scattering interaction although not with quite as high an efficiency in energy conversion as protons in an organic scintillator. However, it can offer significant advantages over organic scintillators in that the electron density of ^{4}He is low so gamma-ray interaction (i.e. Compton scattering) is much less probable than neutron interaction [22]. ^{4}He tubes are generally of small diameter limiting further the probability of gamma-ray interaction. In regular organic scintillators, gamma-ray interactions depositing the same amount of energy as a charged particle produce more scintillation light but in a noble gas such as ^{4}He, the light produced is essentially the same, i.e. linear to energy deposited irrespective of the origin. Taken together, these advantages greatly facilitate separation of fast neutrons from gamma rays using pulse-shape analysis. Figure 9.13 shows a comparison of the discrimination achievable with a ^{4}He scintillation detector and a comparable organic liquid scintillator detector.

9.2 Thermal neutron detectors

In experimental nuclear physics, fast neutron detection, as discussed above, is the most relevant technique. Thermal neutron detection is of lesser importance since while it can detect the presence of the neutron, by the time the neutron is detected all details on its initial energy and direction of travel are lost. Moreover, depending on the slowing medium, it takes some time for neutrons to thermalise, meaning that it would be difficult to establish prompt coincidences between detection of such neutrons and other radiation emitted when the initial fast neutron was produced. While relevance to nuclear physics is limited, thermal neutron detection is much more important in societal applications and a range of examples are reviewed in section 9.3.

9.2.1 ^{3}He gas-filled proportional counter

The classic thermal neutron detector is a ^{3}He gas-filled proportional counter (also known more commonly as a ^{3}He tube). The physics of gas-filled proportional counters was outlined in section 4.3.1. This is a regime where the electric field within the detector is sufficiently high that avalanche multiplication occurs. As discussed above for fast neutrons, neutrons are not themselves ionising but thermal neutrons

[3] Note that such detectors are based on scintillation and should not be confused with ^{3}He proportional counters for thermal neutron detection discussed in section 9.2.1.

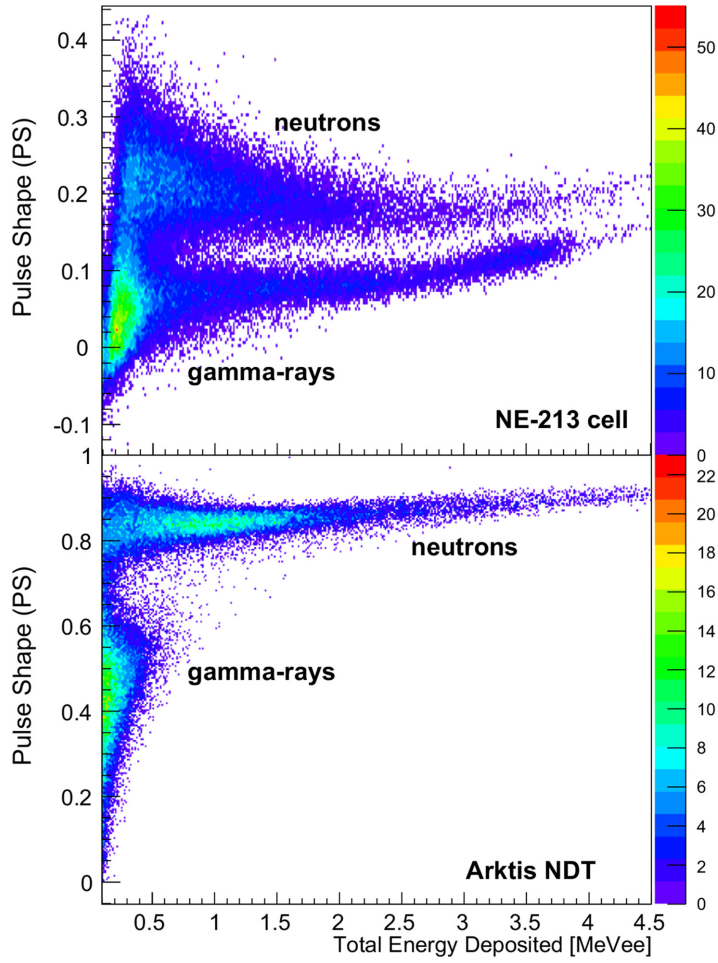

Figure 9.13. Pulse shape parameter as a function of the total energy deposited in an NE-213 liquid scintillator detector (top) and a ^{4}He scintillator detector (bottom). The pulse shape parameter is defined as the ratio of the scintillation-light yield in the tail of the signal to the total. (Reprinted from [22] with the permission of Elsevier under Creative Commons License.)

can interact with ^{3}He to produce light charged particles. The relevant nuclear reaction is

$$n_{\text{th}} + {}^3\text{He} \rightarrow t + p. \tag{9.3}$$

The outgoing proton and triton share the kinetic energy associated with the reaction Q-value (0.764 MeV); it is these light charged particles that ionise the gas and produce a large, proportional signal.

^{3}He detectors have the significant advantage of being largely insensitive to gamma rays. Gamma rays typically interact only at the detector walls and produce small amplitude signals which can be discriminated from the neutron signals by

setting an appropriate electronic threshold. ^{3}He is, however, a scarce commodity and at times in the last decade there have been supply shortages and increased prices, leading to resurgence of interest in ^{3}He replacements, particularly for homeland security which is discussed in more detail in section 9.3.1.

9.2.2 ^{3}He replacements

There are a number of alternatives to ^{3}He leading to detectors with varying efficiencies and associated advantages/disadvantages. Most such alternative detectors are based on the employment of detector materials containing ^{6}Li or ^{10}B which have high thermal neutron cross sections and undergo breakup into energetic charged particles via the following reactions:

- $^{10}\mathrm{B} + n_{\mathrm{th}} \rightarrow {}^{7}\mathrm{Li} + \alpha + 2.31$ MeV
- $^{6}\mathrm{Li} + n_{\mathrm{th}} \rightarrow {}^{3}\mathrm{H} + \alpha + 4.78$ MeV.

The resulting charged particles can ionise a gas or induce scintillation in a solid material.

Boron trifluoride (BF_3)

Boron itself is a solid but boron trifluoride (BF_3) provides a useful alternative to ^{3}He since it makes boron available in a gaseous form. Moreover, it can be enriched with ^{10}B to produce a more efficient detector. BF_3 is used in gas-filled proportional counters where it serves both as the converter material and as the proportional gas. Figure 9.14 shows the typical response of a BF_3 detector; the Q-value of the neutron-converting reaction is evident from the peak around 2.3 MeV. The low-energy tail of the response arises from so-called *wall effects* where one of the reaction products

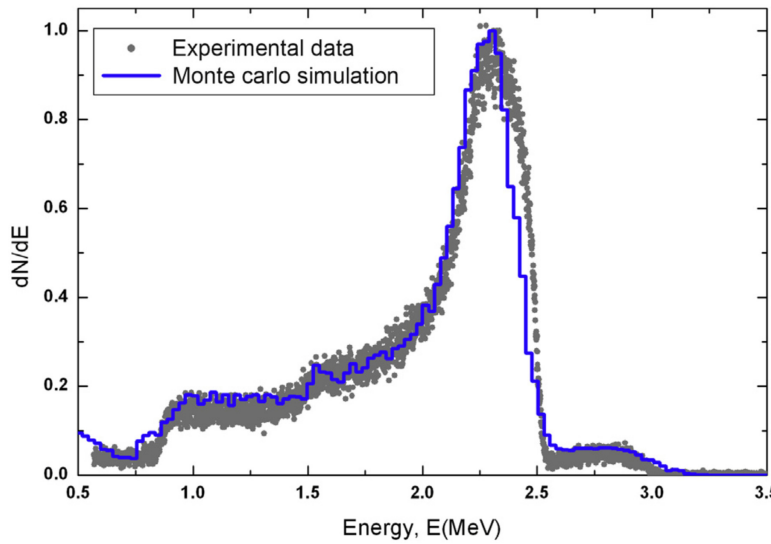

Figure 9.14. Comparison of the experimental response of a typical BF_3 detector with a Monte Carlo simulations. (Reprinted from [23] with the permission of Elsevier under Creative Commons License.)

may hit the detector wall without depositing all its energy in the gas. As with ^{3}He tubes, the gamma-ray component to the detector signal is of low amplitude relative to that from the charged particles and can be readily discriminated. The principal disadvantage of BF_3 is its high toxicity which poses challenges in its handling.

Boron straws

Boron straws are an interesting alternative to both ^{3}He and BF_3 tubes that employ boron converter material in a solid form [24–26]. A boron straw detector comprises one or more gas-filled proportional counters with their walls typically covered with a 1 μm thickness of B_4C, highly enriched in ^{10}B (see figure 9.15). The light charged particles, ^{7}Li and α from the neutron-conversion reaction enter the gas volume and ionise it. The proportional gas is typically a mixture (90/10 by volume) of Ar/CO_2 at low pressure (0.7 atm) [26]. Such a gas mixture is intrinsically safe compared to BF_3 discussed above. Since the particles are not produced directly in the gas volume, there is potential for them to be emitted in the wrong direction or to be stopped within the conversion layer itself due to their short range. This is what dictates the maximum thickness of the conversion layer that can be employed. To increase the effective surface area of the conversion layer and, hence, the thermal neutron detection efficiency, complex star-shaped tube geometries have been explored [24].

^{6}Li-doped scintillating glass

Glasses are an excellent detector medium because of their robustness and resistance to melting [27]. ^{6}Li-doped scintillating glasses are a well-established technology which can be competitive in some cases with ^{3}He tubes depending on the application [28]. They are available from manufacturers such as Scintacor. Typical lithium content of the scintillating glass is around 7% of which the ^{6}Li component can be enriched to 95%. The glasses are doped with cerium to improve the scintillation light output. Discrimination of thermal neutrons from gamma rays is carried out on the basis of the pulse amplitude since the energy deposited in the break-up of ^{6}Li

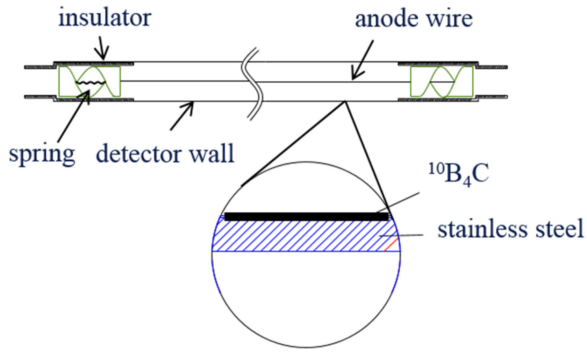

Figure 9.15. Design of a boron straw detector. Each tube is an 8.0 mm diameter proportional counter with 800 mm sensitive length. The detector is formed of stainless steel with 0.2 mm thickness. All tubes have been heated under high temperature for outgassing. An electrophoresis method is used to coat the inner walls with B_4C (90% ^{10}B enrichment). (Reprinted from [25] with the permission of IOP Publishing.)

following interaction with a thermal neutron is large in comparison to typical energy deposited in the glass through Compton scattering etc. A way in which gamma-ray discrimination can be improved is to operate a ^{6}Li-enriched detector in parallel with a ^{6}Li-depleted detector and compare the signal.

Sandwiched converter layers

The light charged particles produced in the ^{6}Li and ^{10}B thermal neutron-conversion reactions are emitted in a roughly back-to-back geometry in order to conserve momentum, and will have a short range in matter. These features have been exploited to produce thermal neutron detectors by sandwiching a ^{6}LiF film or ^{10}B layer between two silicon detectors [29] or two diamond detectors [30]. The efficiency in such applications is naturally limited by the dimensions, particularly the limited thickness of the converter layer.

Loaded plastic scintillator

Plastic scintillator (see section 9.1.2) can be converted into a high efficiency thermal neutron detector by loading it with suitable materials such as gadolinium, lithium or boron, which have each have isotopes high cross-sections for thermal neutrons. A gadolinium-doped plastic scintillator functions via neutron capture principally onto the component isotopes such as ^{155}Gd and ^{157}Gd, the latter of which has a thermal neutron capture cross section of 257 000 barns—the highest of any stable isotope [31]. The relevant reaction is

$$^{157}\mathrm{Gd} + n_{\mathrm{th}} \rightarrow ^{158}\mathrm{Gd} + 7.94\ \mathrm{MeV}. \tag{9.4}$$

The excess energy is released as a cascade of gamma rays for which the probability of at least one of them interacting in the plastic is high.

Boron-loaded [32] and lithium-loaded [33] plastic scintillators function by thermal neutron capture on to ^{10}B and ^{6}Li, respectively, which leads to energetic ionising charged-particles within the plastic. Figure 9.16 provides an example of pulse shape

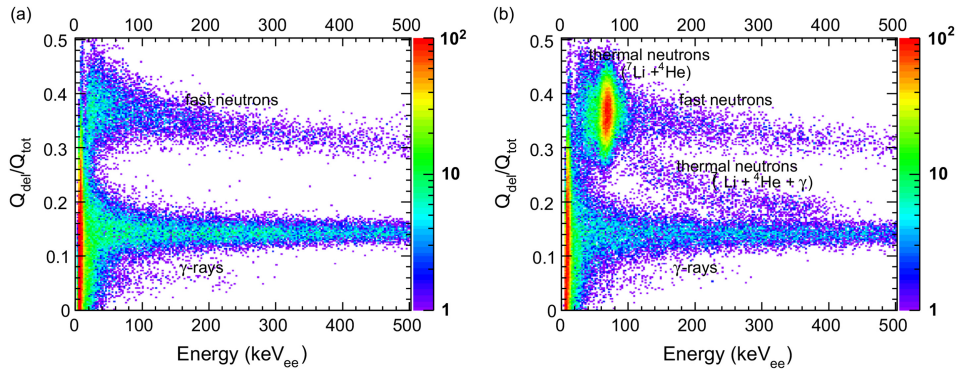

Figure 9.16. Pulse shape discrimination with different plastic scintillators: (left) regular pulse-shaping discriminating plastic (cf figure 9.12) and (right) borated plastic scintillator containing 5% by weight of m-carborane with natural boron abundance. The signature of the breakup of ^{10}B is clearly seen in the top left of the plot. (Reprinted from [32] with the permission of Elsevier.)

discrimination of thermal neutrons using a borated plastic where the thermal events are seen to be very well localised [32].

9.3 Industrial and security applications of neutron detection

There are a limited number of societal applications of neutron detection chiefly in the industrial and homeland security sectors.

9.3.1 Homeland security

There are very few natural sources of neutrons in our environment so detection of even a low counting rate of neutrons can be indicative of the presence in the locality of a fission neutron source. This is obviously of high interest in terms of nuclear security where special nuclear materials such as uranium and plutonium are under tight control.

Portal monitors

Radiation portal monitors (RPMs) are commonly found at ports and airports to identify illicit transport of special nuclear materials. Traditionally, such RPMs contain ^{3}He detectors, surrounded by moderating material such as polyethylene, to detect thermal neutrons; figure 9.17 shows an example of such a conventional radiation portal monitor (RPM). The choice of ^{3}He for this application arises from

Figure 9.17. Two ^{3}He tubes mounted within neutron-moderating material as a radiation portal monitor (RPM). (Reprinted from [34] with the permission of Elsevier.)

its high cross-section for thermal neutrons and from the fact that is largely insensitive to gamma rays as a background. There is high interest, as discussed above, in finding cost-effective ^{3}He replacements.

Handheld/wearable thermal neutron detectors

The Kromek D3S offers simultaneous thermal neutron detection and gamma-ray detection. This unit was already described in section 7.1.1 in terms of its ability to identify radioisotopes and map their location. The thermal neutron capability is provided by a layer of scintillator (zinc sulphide) mixed with ^{6}LiF converter material. The scintillation light is collected by a silicon photomultiplier. This sensor

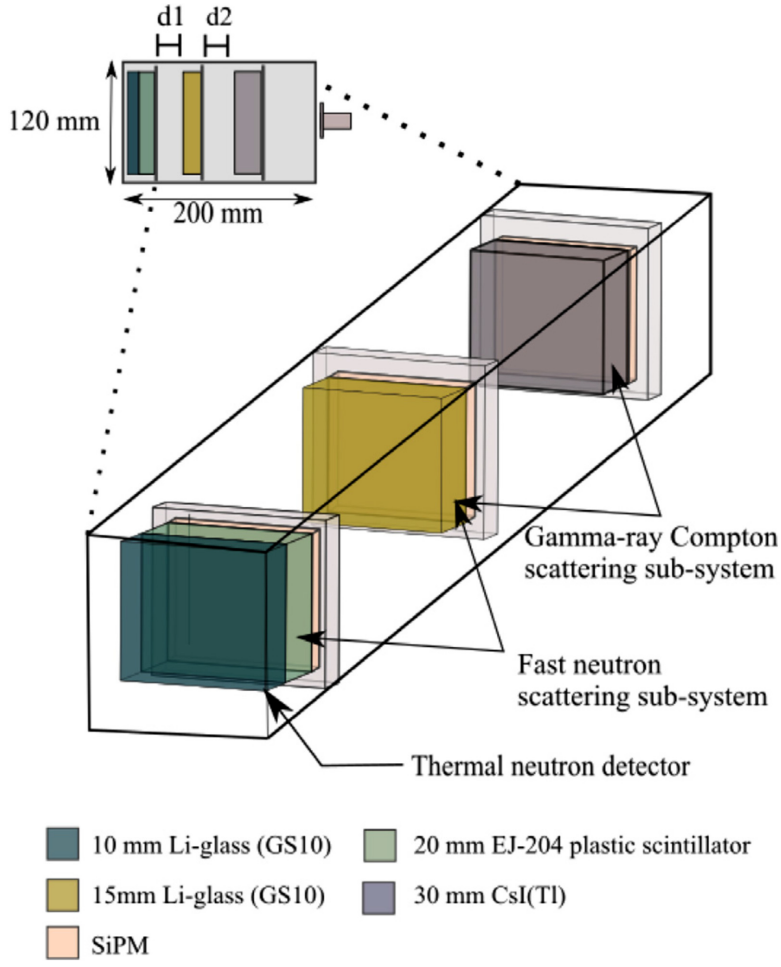

Figure 9.18. Diagram of a hand-held neutron/gamma-ray imager with three separate detector planes. The detector components are labelled on the diagram (see text for details). (Reprinted from [35] with the permission of Elsevier under Creative Commons License.)

is intrinsically thin and has high rejection of background from other sources such as gamma rays.

Al Hamrashdi *et al* [35] report on the development of a handheld imager which would measure both thermal and fast neutrons as well as gamma rays—see figure 9.18. It uses an elaborate series of three detector planes comprising different detector materials which draws together many of the concepts discussed in this chapter as well those in chapter 5. The first detector plane (closest to the neutron source) has two detector slabs optically coupled: a 10mm thickness of ^{6}Li-doped glass and a 20 mm thickness of plastic scintillator. The second detector plane comprises a further 15 mm thick slab of ^{6}Li-doped glass while the third and final detector plane is 30 mm thickness of CsI(Tl). Each detector plane is instrumented with an 8 × 8 array of SensL J-series SiPMs (see section 5.3.3). With these thin slabs of scintillator, the location where the scintillation light is detected is closely correlated with the position in the slab where the light is generated.

The detector shown in figure 9.18 is designed to identify thermal neutrons in the front of the first detector plane. The rear of the first detector plane serves as a fast neutron scatter and the scattered neutrons are detected in the second detector plane (see figure 9.19). This second plane doubles up as a Compton scattering plane for gamma rays where the scattered gamma rays are detected in the third detector plane, functioning as a Compton camera—a technique described in section 7.1.2.

9.3.2 Borehole logging

Thermal neutron detection is employed in borehole logging for porosity measurements. This reflects the fact that the scattering and thermalisation of neutrons is highly material dependent; moderation of neutrons will occur much more rapidly in hydrogen-rich material such as water-filled cavities than in solid rock. The porosity

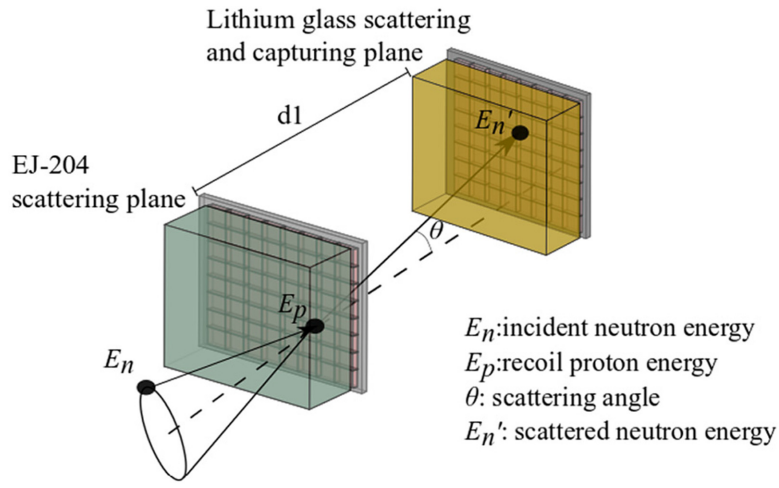

Figure 9.19. Concept of a plastic scintillator and ^{6}Li-doped detector plane as a neutron-scatter imaging detector. (Reprinted from [35] with the permission of Elsevier under Creative Commons License.)

measurements are implemented using a sealed ^{241}Am–Be neutron source in the neutron probe. Two ^{3}He proportional detectors are mounted sequentially along the borehole probe away from the source. The ratio of the thermal neutron flux reaching the near and far detectors depends on the hydrogen-content and porosity. Using two detectors with this ratio method provides a porosity measurement which is independent of borehole diameter.

References

[1] Birks J B 1964 *The Theory and Practice of Scintillation Counting* (International Series of Monographs on Electronics and Instrumentation vol 2) 1st edn (Oxford: Pergamon)

[2] Brooks F D 1979 Development of organic scintillators *Nucl. Instrum. Methods* **162** 477–505

[3] Schuster P 2016 Investigating the anisotropic scintillation response in anthracene through neutron, gamma-ray and muon measurements *IEEE Trans. Nucl. Sci.* **63** 1942

[4] Birks J B 1951 Scintillations from organic crystals: specific fluorescence and relative response to different radiations *Proc. R. Soc.* A **64** 874

[5] Ogawa T, Yamaki T and Sato T 2018 Analysis of scintillation light intensity by microscopic radiation transport calculation and Förster quenching model *PLoS One* **13** e0202011

[6] Yanagida T, Watanabe K and Fujimoto Y 2015 Comparative study of neutron and gamma-ray pulse shape discrimination of anthracene, stilbene and p-terphenyl *Nucl. Instrum. Methods* A **784** 111–4

[7] Garrett P E 2014 DESCANT—the deuterated scintillator array for neutron tagging *Hyperfine Interact* **225** 137–41

[8] Valiente-Dobon J J *et al* 2019 NEDA—NEutron Detector Array *Nucl. Instrum. Methods Phys. Res.* A **927** 81–6

[9] Wong J *et al* 2014 The DEuterated SCintillator Array for Neutron Tagging *EPJ Web Conf.* **66** 11040

[10] Garrett P E 2014 The evolving structure of the Cd isotopes *EPJ Web Conf.* **66** 02039

[11] Skeppstedt O *et al* The EUROBALL neutron wall–design and performance tests of neutron detectors *Nuclear Instrum. Methods Phys. Res.* A **421** 531–41

[12] Moser S W, Harder W F, Hurlbut C R and Kusner M R 1993 Principles and practice of plastic scintillator design *Radiat. Phys. Chem.* **41** 31–6

[13] Hajagos T J, Liu C, Cherepy N J and Pei Q 2018 High-Z sensitized plastic scintillators: a review *Adv. Mater.* **30** 1706956

[14] Giot M *et al* 2017 Nuclear instrumentation and measurement: a review based on the ANIMMA conferences *EPJ Nucl. Sci. Technol.* **3** 33

[15] Son J, Kim D G, Lee S, Park J, Kim Y, Schaarschmidt T and Kim Y K 2018 Improved 3D printing plastic scintillator fabrication *J. Korean Phys. Soc.* **73** 887–92

[16] Nusrat H, Pang G, Ahmad S B, Keller B and Sarefehnia A 2019 Quantifying the impact of lead doping on plastic scintillator response to radiation *Med. Phys.* **46** 4215–23

[17] Peters W A *et al* 2016 Performance of the versatile array of neutron detectors at low energy (VANDLE) *Nucl. Instrum. Methods* A **836** 122–33

[18] Douma C A *et al* 2017 Design studies for the NeuLAND VETO detector *J. Phys.: Conf. Ser.* **1024** 012027

[19] Zaitseva N P, Glenn A M, Mabe A N, Carman M L, Hurlbut C R, Inman J W and Payne S A 2018 Recent developments in plastic scintillators with pulse shape discrimination *Nucl. Instrum. Methods* A **889** 97–104

[20] Cieslak M J, Gamage K A A and Glover R 2019 Critical review of scintillating crystals for neutron detection *Crystals* **9** 480
[21] Chandra R, Davatz G, Friedrich H, Gendotti U and Murer D 2012 Fast neutron detection with pressurized ^{4}He scintillation detectors *J. Instrum.* **7** C03035
[22] Jebali R *et al* 2015 A first comparison of the responses of a ^{4}He-based fast-neutron detector and a NE-213 liquid-scintillator reference detector *Nucl. Instrum. Methods* A **794** 102–8
[23] Nasir R, Aziz F, Mirza S M and Mirza N M 2018 Experimental and theoretical study of BF_3 detector response for thermal neutrons in reflecting materials *Nucl. Eng. Technol.* **50** 439–45
[24] Lacy J L, Athanasiades A, Martin C S, Sun L and Vazquez-Flores G L 2013 The evolution of neutron straw detector applications in homeland security *IEEE Trans. Nucl. Sci.* **60** 1140–6
[25] Jiang Z G, Gong H, Li J M, Wang Y Q and Wang X W 2018 Experimental study of a boron coated straw detector module at CPHS *J. Instrum.* **13** P08004
[26] Klausz M *et al* 2019 Performance evaluation of the boron coated straws detector with Geant4 *Nucl. Instrum. Methods* A **943** 162463
[27] Bollinger L M, Thomas G E and Ginther R J 1962 Neutron detection with glass scintillators *Nucl. Instrum. Methods* **17** 97–116
[28] Xu M, Tang Z-C, Chen G-M and Tao J-Q 2013 Comparison of thermal neutron detection efficiency of ^{6}Li scintillation glass and ^{3}He gas proportional tube *Chinese Phys.* C **37** 106001
[29] Omar A *et al* 2019 Development of a handheld thermal neutron detector (GAMBE) using stacked silicon sensors coated with ^{6}LiF films *Radiat. Meas.* **129** 106180
[30] Almaviva S *et al* 2010 Improved performance in synthetic diamond neutron detectors: Application to boron neutron capture therapy *Nucl. Instrum. Methods* A **612** 580–2
[31] Ovechkina L, Riley K, Miller S, Bell Z and Nagarkar V 2009 Gadolinium loaded plastic scintillators for high efficiency neutron detection *Phys. Proc.* **2** 161–70
[32] Pawelczak I A, Glenn A M, Martinez H P, Carman M L, Zaitseva N P and Payne S A 2014 Boron-loaded plastic scintillator with neutron-gamma pulse shape discrimination capability *Nucl. Instrum. Methods* A **751** 62–9
[33] Mabe A N, Glenn A M, Carman M L, Zaitseva N P and Payne S A 2016 Transparent plastic scintillators for neutron detection based on lithium salicylate *Nucl. Instrum. Methods* A **806** 80–6
[34] Kouzes R T *et al* 2010 Neutron detection alternatives to ^{3}He for national security applications *Nucl. Instrum. Methods* A **623** 1035–45
[35] Al Hamrashdi H, Cheneler D and Monk S D 2020 A fast and portable imager for neutron and gamma emitting radionuclides *Nucl. Instrum. Methods* A **953** 163253